

A STUDY ON DEBRIS FLOW OUTFLOW DISCHARGE AT A SERIES OF SABO DAMS

Namgyun Kim * · Hajime NAKAGAWA ** · Kenji KAWAIKE *** ·
Hao ZHANG ****

A STUDY ON DEBRIS FLOW OUTFLOW DISCHARGE AT A SERIES OF SABO DAMS

Namgyun K_{IM}^{*}, Hajime N_{AKAGAWA}^{**},
Kenji K_{AWAIKE}^{***} and Hao Z_{HANG}^{****}

Abstract

Debris flows are very dangerous phenomena in mountainous areas. Sabo dams are commonly used to mitigate debris flows and they are effective countermeasures against debris flow disasters. However, human life and property remain at risk off debris flows. In order to develop measures to increase the effectiveness of a Sabo dam, its control function and design have been reported. Nevertheless, few studies have discussed the control functions of a series of Sabo dams. This paper estimates debris flow discharges at a Sabo dam site using overflow equations. A 1-D numerical simulation method of debris flows is presented. Numerical simulations of debris flow were conducted including overflow discharge at the dam point and laboratory experiments were performed to validate the simulation results. Comparisons between the numerical simulation results and laboratory experimental results show reasonable agreement. Application of the numerical model used here is recommended to calculate overflow discharge at Sabo dam sites and to evaluate the sediment capturing effects of Sabo dam arrangements.

Key words : debris flow, Sabo dam, overflow equation, deposition, numerical simulation

* Student Member of JSNDS, Doctoral Student, Department of Civil and Earth Resources Engineering, Kyoto University (Katsura Campus, Nishikyo-ku, Kyoto 615-8540, JAPAN)

** Member of JSNDS, Dr. of Eng., Prof., DPRI, Kyoto University (Yoko-oji, Fushimi, Kyoto 612-8235, JAPAN)

*** Member of JSNDS, Dr. of Eng., Assoc. Prof., DPRI, Kyoto University (Yoko-oji, Fushimi, Kyoto 612-8235, JAPAN)

**** Member of JSNDS, Dr. of Eng., Assist. Prof., DPRI, Kyoto University (Yoko-oji, Fushimi, Kyoto 612-8235, JAPAN)

1. INTRODUCTION

Many types of sediment-related disasters occur in mountainous areas (Fig. 1). Sediment-related disasters are caused by localized torrential downpours, earthquakes, volcanic eruption, and so forth. These are natural phenomena. However, as urbanization continues to expand in mountainous areas, the risk of sediment-related disasters is increasing. In particular, debris flows frequently cause extensive damage to property and loss of life.

Debris flows are generally initiated from upstream of a mountainous area when unconsolidated material becomes saturated and unstable or originate directly from landslides. They can flow down several kilometers and damage the residential areas at the foot of mountains. They contain various particle sizes from fine material to large boulders and these large boulders accumulate at the front part of the flow. Thus damage caused by debris flow can be severe. In addition debris flows can cause morphological changes, serious casualties and damage to property. Figure 2 shows the number of debris flow occurrences from 2000 to 2012 in Japan.

Countermeasures designed to reduce debris flow disasters are classified into structural and non-structural measures. Structural measures include Sabo dams, guide levees and training channels, while non-structural measures include warning systems, proper land use in the areas and the

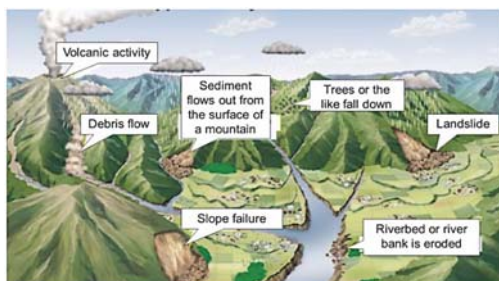


Fig.1 Sediment-related disasters (Photo source : DPWH, Japan)

reinforcement of houses etc. Sabo dams are an effective structural countermeasure to control debris flow. They play an important role in the management and development of a river basin. Sabo dams can be distinguished into two types: closed and open dams (Di Silvio., 1990; Armanini et al., 1991). Closed-type Sabo dams intercept debris flow to the downstream. In contrast, open-type Sabo dams are constructed with suitable openings in the body of the structure. Therefore part of the sediment is allowed to pass through. These two types of Sabo dams are constructed in series along the channel.

The advance of science and technology has led to more advantageous countermeasures for mitigating debris flow damage. To increase the effectiveness of Sabo dams, the control functions of such dams have been reported. Such Sabo dam functions have been described in many laboratory experimental studies and numerical simulation studies (Honda et al., 1997; Imran, J. et al., 2001). Also, considerable theoretical and numerical works have been performed on the size, shape and structure of Sabo dams (Mizuyama et al., 1988; Johnson et al., 1989). These studies contribute to technical standard guidelines on debris flows. Thus, there are studies on methods of evaluating the control function of a series of Sabo dams (Osti et al., 2008). However, further studies are required

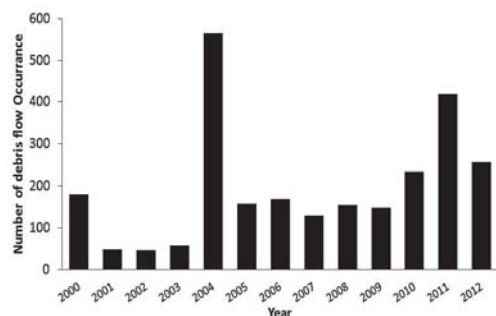


Fig.2 The number of debris flow occurrence in Japan (Data source : MLIT, Japan)

to develop general guidelines on a series of Sabo dams. Few studies have reported about control functions of a series of Sabo dams.

This paper describes a methodological approach for estimating debris flow discharge at a series of Sabo dams, and proposes equations for evaluating the effectiveness of a series of closed-type Sabo dams. A 1-D numerical model of debris flow is presented. Numerical simulations were conducted including debris flow overflow at the dam point and analyzed with boundary conditions. To verify the suggested numerical model, laboratory experiments were performed.

The numerical model is used to study the effect of Sabo dam arrangement. Through the proposed calculation method of overflow discharge at the dam point, determination of optimal distance between Sabo dams is expected.

2. NUMERICAL MODEL

2.1 Governing Equations

(1) Transport and bed surface elevation equations

Debris flows are a fluid mixture that consists of granular materials and water. The equations used are the depth averaged one-dimensional momentum and continuity equations. The equations for the mass conservation of sediment-water mixture and mass conservation of sediment are as follows.

Momentum equation of sediment and water flow mixture:

$$\frac{\partial M}{\partial t} + \beta \frac{\partial(uM)}{\partial x} = gh \sin \theta_b - gh \cos \theta_b \frac{\partial h}{\partial x} - \frac{\tau_b}{\rho_T} \quad (1)$$

Continuity equation of flow mixture:

$$\frac{\partial h}{\partial t} + \frac{\partial M}{\partial x} = i \quad (2)$$

Continuity equation of sediment particles:

$$\frac{\partial(C_h)}{\partial t} + \frac{\partial(CM)}{\partial x} = iC_* \quad (3)$$

where, $M (= uh)$ is the x components of the flow flux, x is the flow direction coordinate, t is time, β is the momentum correction factor equal to 1.25 for a stony debris flow (Takahashi et al., 1992), u is the components of mean velocity, g is the acceleration of gravity, h is flow depth, θ_b is the bed slope, τ_b is components of the resistance to flow, ρ_T is mixture density ($\rho_T = \sigma C + (1-C)\rho$), σ is density of the sediment particle, ρ is density of the water, i is erosion (>0) or deposition (≤ 0) velocity, C is the sediment concentration in the flow, C_* is maximum sediment concentration in the bed.

The equation of bed variation due to erosion or deposition is described as follows:

$$\frac{\partial z_b}{\partial t} + i = 0 \quad (4)$$

where, z_b is erosion or deposition thickness of the bed measured from the original bed surface elevation. In the fixed bed, z_b equals 0. Actually, the sediment in the fixed bed should be contained in the flow parts when erosion occurs. However there is no sediment in the fixed bed.

(2) Erosion and deposition velocity equations

The erosion and deposition i are source terms. The velocity equations that have been given by Takahashi et al. (1992) are described as follows:

Erosion velocity, if $C < C_*$;

$$i = \delta \frac{C_\infty - C}{C_* - C_\infty} \frac{M}{d_m} \quad (5)$$

Deposition velocity, if $C \geq C_*$;

$$i = \delta' \frac{C_\infty - C}{C_*} \frac{M}{d_m} \quad (6)$$

where, δ is erosion coefficient, δ' is deposition

coefficient, d_m is mean diameter of sediment, and C_∞ is the equilibrium sediment concentration described as follows (Nakagawa et al., 2003).

If $\tan\theta_w > 0.138$, a stony type debris flow occurs, and

$$C_\infty = \frac{\rho_m \tan \theta_w}{(\sigma - \rho_m)(\tan \phi - \tan \theta_w)} \quad (7)$$

If $0.03 < \tan\theta_w \leq 0.138$, an immature type of debris flow occurs, and

$$C_\infty = 6.7 \left\{ \frac{\rho_m \tan \theta_w}{(\sigma - \rho_m)(\tan \phi - \tan \theta_w)} \right\}^2 \quad (8)$$

If $\tan\theta_w \leq 0.03$, a turbulent water flow with bed load transport occurs, and

$$C_\infty = \frac{(1 + 5 \tan \theta_w) \tan \theta_w}{\frac{\sigma}{\rho_m} - 1} \left(1 - \alpha_0^2 \frac{\tau_{*c}}{\tau_*} \right) \left(1 - \alpha_0^2 \sqrt{\frac{\tau_{*c}}{\tau_*}} \right) \quad (9)$$

$$\alpha_0^2 = \frac{2\{0.425 - (\sigma/\rho_T) \tan \theta_w / (\sigma/\rho_T - 1)\}}{1 - (\sigma/\rho_T) \tan \theta_w / (\sigma/\rho_T - 1)} \quad (10)$$

$$\tau_{*c} = 0.04 \times 10^{1.72 \tan \theta_w} \quad (11)$$

$$\tau_* = \frac{h \tan \theta_w}{(\sigma/\rho_T - 1)d_m} \quad (12)$$

where, θ_w is water surface gradient, ρ_m is density of the interstitial muddy fluid, ϕ is internal friction angle of the sediment τ_{*c} is the non-dimensional critical shear stress and τ_* is the non-dimensional shear stress.

(3) Bottom shear stress equations

The resistance terms are given by the following equations for a stony debris flow:

$$\tau_b = \frac{\rho_T}{8} \left(\frac{d_m}{h} \right)^2 \frac{u|u|}{\{C + (1-C)\rho/\sigma\} \{(C_\infty/C)^{1/3} - 1\}^2} \quad (13)$$

An immature debris flow occurs when C is less than $0.4C_\infty$, and the bottom shear stress is described as follows:

$$\tau_b = \frac{\rho_T}{0.49} \left(\frac{d_m}{h} \right)^2 u|u| \quad (14)$$

In the case of turbulent flow, the Manning's equation is used to determine the bottom shear stress. When C is less than 0.02,

$$\tau_b = \frac{\rho g n^2 u|u|}{h^{1/3}} \quad (15)$$

where, n is the Manning resistance coefficient.

2.2 Conditions of Sabo Dam

The closed-type Sabo dam is set at the grid line where discharge is calculated (Fig. 3). The grid size is 5 cm. The flow surface gradient, θ_w , and bed gradient, θ_b , are calculated at the center of the cell. The flow surface gradient θ_w and bed gradient θ_b are calculated by the average of each value of $\theta_{w, i-1}$, $\theta_{b, i-1}$ and $\theta_{w, i+1}$, $\theta_{b, i+1}$. However, if there is a Sabo dam, the calculation method is changed as follows:

Gradient at the dam point ($z_i < z_{dam}$);

$$\theta_b = \tan^{-1} \frac{z_i - z_{i+1}}{\Delta x} \quad (16)$$

$$\theta_w = \tan^{-1} \frac{z_i - z_{i+1} + h_i - h_{i+1}}{\Delta x} \quad (17)$$

Gradient at the dam point ($z_i \geq z_{dam}$);

$$\theta_b = \tan^{-1} \frac{z_i - z_{i+1}}{2\Delta x} \quad (18)$$

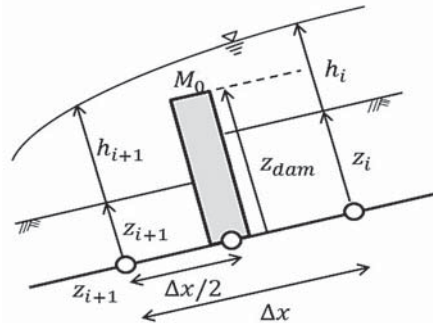


Fig.3 Definition of the variables

$$\theta_w = \tan^{-1} \frac{z_i - z_{i+1} + h_i - h_{i+1}}{24x} \quad (19)$$

2.3 Overflow Equations

Sabo dams involve obstructing the path of flow. This is a vertical obstruction over which the debris must flow such as a weir. At that time, outflow discharge at the dam point can be calculated using certain equations. To calculate debris flow discharge at the dam point, the overflow equation and free overfall equation are applied.

Overflow equation (Complete flow):

$$\left(\frac{h_{i+1}}{h_i} \leq \frac{2}{3}\right) \quad M_0 = ch_i \sqrt{2gh_i} \quad (20)$$

Overflow equation (Incomplete flow):

$$\left(\frac{h_{i+1}}{h_i} > \frac{2}{3}\right) \quad M_0 = ch_{i+1} \sqrt{2g(h_i - h_{i+1})} \quad (21)$$

Free overfall equation:

$$(h_i > Z_{dam}) \quad M_0 = ch_i \sqrt{gh_i} \quad (22)$$

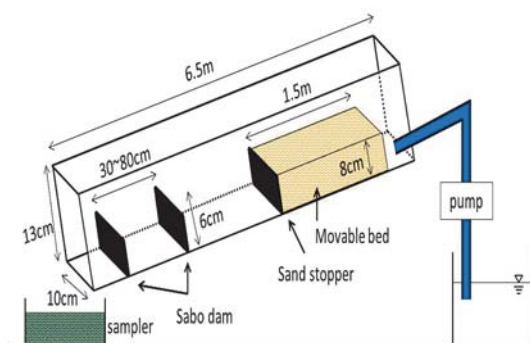
where, M_0 is debris flow discharge per unit width at the dam point, and c is the overflow coefficient. As the overflow equation and free overfall equation are adjusted at the dam point, flow conditions are changed by the bed elevation (Table 1).

3. LABORATORY EXPERIMENTS

Figure 4 shows the experimental flume setup. The laboratory experiments were conducted using a rectangular flume, which is 6.5m long, 13 cm high, 10 cm wide and has an incline of 18°. The flume is divided into two parts by an 8cm high sand stopper that is installed 1.5m from the upstream end of the flume. The upstream part is filled with a movable bed that consists of silica sand and gravel

Table 1 Flow conditions at Sabo dam

	Condition	Calculated M_0
Flow 1	$z_i + h_i \leq z_{dam}$	0
Flow 2	$z_i + h_i > z_{dam}$ $z_i < z_{dam}$ $z_{i+1} + h_{i+1} \leq z_{dam}$	Overflow equation (Complete flow) (Equation. 20)
Flow 3	$z_i + h_i > z_{dam}$ $z_i < z_{dam}$ $z_{i+1} + h_{i+1} > z_{dam}$	Overflow equation (Complete flow, Incomplete flow) (Equation. 20,21)
Flow 4	$z_i + h_i > z_{dam}$ $z_i \geq z_{dam}$ $z_{i+1} + h_{i+1} \leq z_{dam}$	Free over fall equation (Equation. 22)
Flow 5	$z_i + h_i > z_{dam}$ $z_i \geq z_{dam}$ $z_{i+1} + h_{i+1} > z_{dam}$	Momentum equation (Equation. 1)



(a) Sketch of experimental setup



(b) Experimental flume

Fig.4 Experimental flume setup

mixtures. The movable bed was set 20cm upstream from the upstream end of the flume, length 150 cm, 8 cm high, and 10 cm wide. Sediment materials with mean diameter $d_m=2.86mm$, maximum diameter $d_{max}=15mm$ and density $\sigma=2.65g/cm^3$, internal friction angle of a sediment $\tan\phi=0.7$ were used. The particle size distribution of the movable bed is shown in Figure 5.

To generate the debris flow, the movable bed is saturated by seepage flow. After fully saturating the movable bed, the debris flow is generated through supplying clear water. The debris flow developed in the experiments is fully stony type debris flow and larger particles are accumulated at the forefront of the debris flow. This debris flow, overtopping the sand stopper, reaches the downstream part of the flume. After overtopping the two Sabo dams, debris flows are captured by the sampler.

The experimental conditions are shown in Table 2. Two closed-type Sabo dams 6 cm high, 10 cm

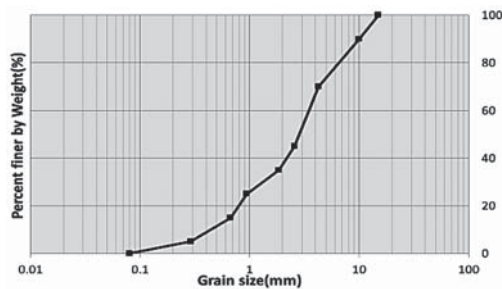


Fig. 5 Particle size distribution of sediment materials

Table 2 Experimental conditions

Experiment No.	Supply water Discharge (cm ³ /s)	Time (sec)	Distance between two Sabo dams (cm)
Case A	300	20	30
Case B			55
Case C			80

wide and 1 cm thick were used for the experiments. The lower Sabo dam was set 30 cm upstream from the downstream end of the flume the upper Sabo dam was set 30 cm, 55 cm, 80 cm upstream from the lower Sabo dam.

Two runs were conducted under the same experimental conditions in order to obtain reliable data. Debris flow discharge and sediment concentration at each dam point were measured using sampler. Debris flow deposition upstream of the Sabo dam was measured by video camera and the images were analyzed over time.

4. RESULTS AND DISCUSSION

The numerical simulations were conducted to calculate debris flow discharge at the dam point and experiments were also performed to validate the numerical model.

Figure 6 shows the simulated results and experimental results of debris flow discharge and sediment concentration. In this graph, time 0 means the start time to supply clear water. The start time of blue line means the time the debris flow reached the upper Sabo dam. Table 3 shows the time the debris flows reached each position.

In Case A, the overflow time of debris flow at the lower Sabo dam is earlier than in Case B and Case C. The distance between two Sabo dams is not sufficient capture debris flow. Sufficient distance

Table 3 Debris flow time (unit : sec)

No.	Case. A		Case. B		Case. C	
	Exp	Sim	Exp	Sim	Exp	Sim
Time to reach upper Sabo dam	12.1	12.3	11.8	12.0	11.6	11.7
Overflow time in upper Sabo dam	12.7	12.6	12.8	12.7	12.5	12.3
Overflow time in lower Sabo dam	14.3	14.1	15.4	15.2	15.5	15.1

between two Sabo dams means that the length between two Sabo dams is longer than the deposition length upstream of one Sabo dam. This deposition starting from the Sabo dam to the

deposition height is equal to 0.

Table 4 shows the debris flow peak discharge. In the experimental results, debris flow discharge is calculated at the downstream end of the flume

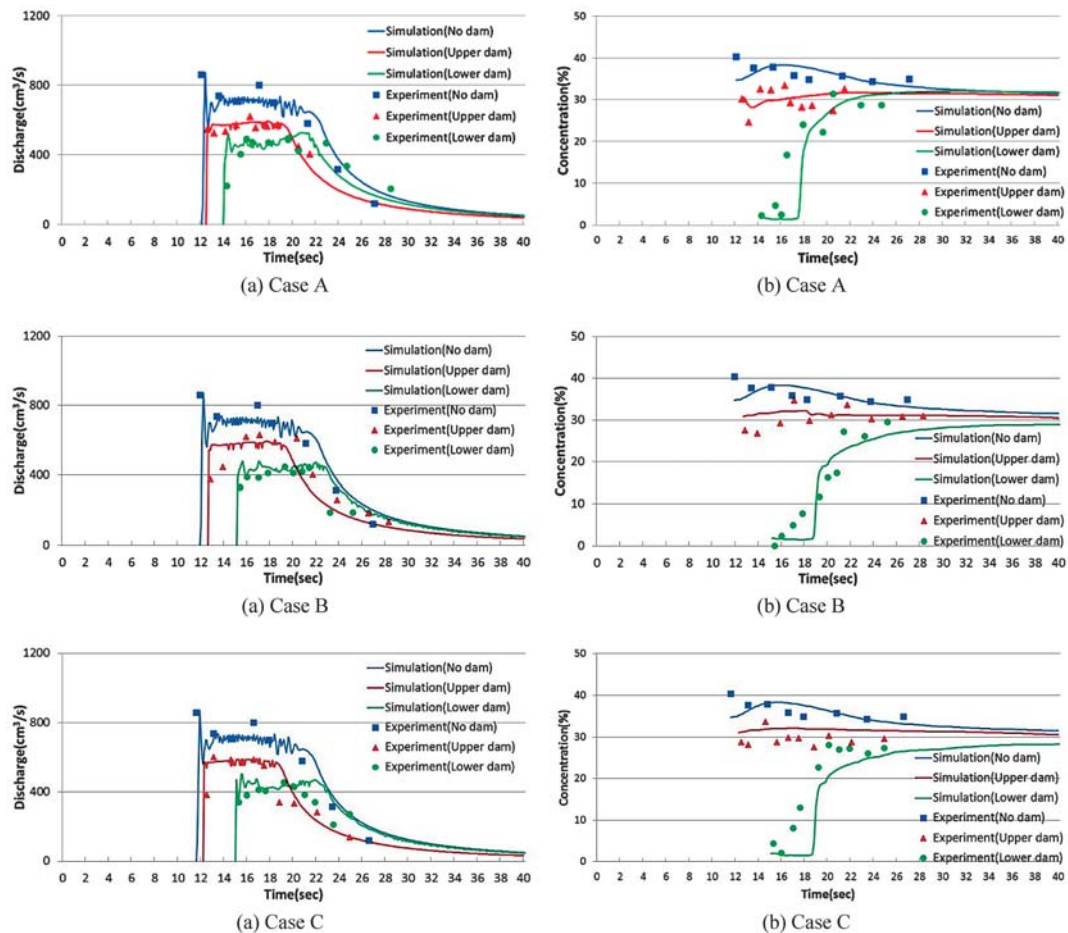


Fig .6 Debris flow discharge (a) and sediment concentration (b)

Table 4 Debris flow peak discharge

(unit : cm³/s)

	No dam		Case A				Case B				Case C			
	Exp	Sim	Exp		Sim		Exp		Sim		Exp		Sim	
			up	low	up	low	up	low	up	low	up	low	up	low
Peak discharge	872	851.19	619.0	409.5	572.9	517.9	629.9	447.3	581.6	447.8	588.2	413.6	587.9	503.7
Decrease Rate (%)	-	-	29.1	14.8	32.8	6.5	27.9	20.9	31.8	15.7	32.6	20.1	31.1	26.4
Total decrease Rate (%)	-	-	43.9		39.3		48.8		47.5		52.7		57.5	

under the no Sabo dam case. Simulated results of debris flow discharge are consistent with the experimental results. Through the series of Sabo dams, the total discharge of debris flow and peak discharge is decreased.

The total average peak discharge rate is 48.4% in the experimental results and 48.1% in the simulation results. However, the longer the distance between two Sabo dams, the higher the rate of total discharge decrease. The situation is different in the lower Sabo dam. The longer the distance between two Sabo dams, the easier it is to form a fully developed debris flow.

The average decrease rate of the upper Sabo dam is 29.8% in the experimental results and 31.9% in the simulation results. However, the average decrease rate of the lower Sabo dam is 18.6% in the experimental results and 16.2% in the simulation results. The efficiency of the decrease rate of debris flow peak discharge at the lower Sabo dam is less than the upper Sabo dam. The reason for this is the sediment concentration. In the Figure 6(b), as debris flows pass the Sabo dam, sediment concentration decreased. First, the sediment concentration is consistent at around 35%. As the debris flows passed the upper Sabo dam, sediment concentration decreased to around 30% and when passing the lower Sabo dam, sediment concentration further decreased. However, overflowed debris flow at the lower Sabo dam does not have a consistent sediment concentration. The initial sediment concentration is lower than 5%. This means that debris flow that is not fully developed reaches the lower Sabo dam. As debris flows overflow the Sabo dam, sediment is captured by the Sabo dam. Therefore, the forefront of the debris flow has a low sediment concentration.

Figure 7 shows the debris flow deposition upstream of the Sabo dam. In this graph, time 0 means the start time of debris flow being captured by the Sabo dam. Some discrepancies are found in

the shape of the deposition between the simulated results and experimental results. The height of deposition in the experimental results is higher than that in the simulation results. The simulation results are underestimated. Therefore, a more feasible coefficient of erosion velocity and coefficient of deposition velocity are required. Through adjusting the discharge coefficient and erosion, deposition coefficient, the debris flow deposition pattern could be further improved.

In this study the debris flow overflow discharge at a series of Sabo dams was evaluated. The suggested simulation method for calculating debris flow discharge results in good agreement with the experimental results.

5. CONCLUSIONS

The numerical model was developed to simulate the debris flow discharge at the dam point. Laboratory experiments were conducted and good results of debris flow discharge as well as sediment concentration were obtained. Debris flow deposition will be further improved through adjustment of the coefficient.

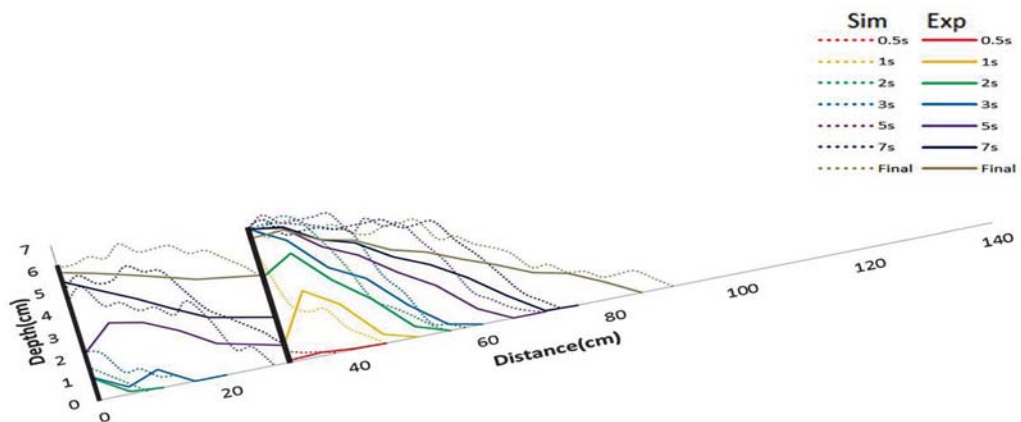
Through considering the combination of Sabo dams, elucidation of technical criteria on the distance between Sabo dam is expected.

ACKNOWLEDGMENT

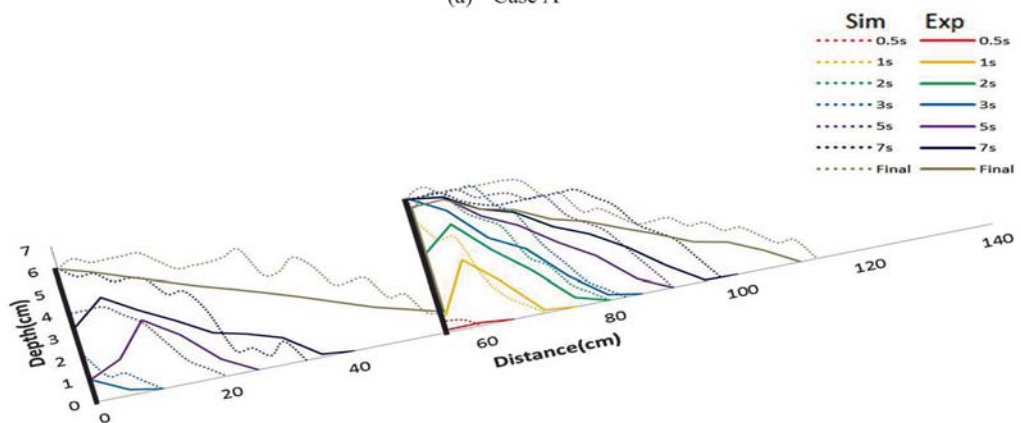
This research was supported by the JSPS AA Science Platform Program (Coordinator: H. Nakagawa) and support of the Wakate fund program by the Kyoto University Global COE Program (GCOE-ARS).

REFERENCES

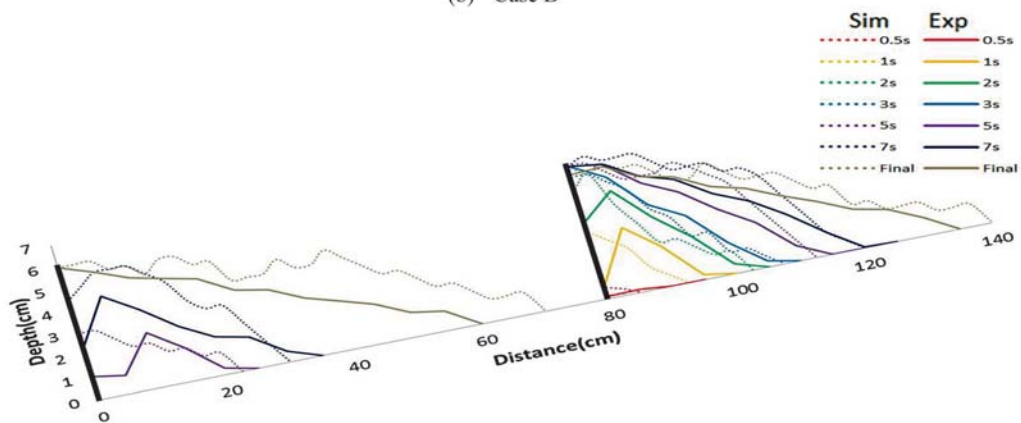
- Armanini A., Dellagiacoma F., and Ferrai L., 1991. From the check dam to the development of functional check dams; Fluvial hydraulics of mountain regions. Lecture notes on Earth Sciences, Vol. 37, Springer, Berlin, 331-344.
- Di Silvio, G., 1991. Soil erosion and conservation Part



(a) Case A



(b) Case B



(c) Case C

Fig. 7 Debris flow deposition upstream of Sabo dam

- 2: Erosion control works. Lecture Notes, IHE, Delft, The Netherlands.
- Honda N., Egashira S., 1997. Prediction of debris flow characteristics in mountain torrents. In Proceedings of 1st International Conference on Debris-flow Hazards Mitigation, ASCE, 707-716.
- Imran J., Gary Parker, Jacques Locat, and Homa Lee., 2001. 1D numerical model of muddy subaqueous and subaerial debris flows. Journal of Hydraulic Engineering, ASCE, Vol. 127, No. 11, 959-968.
- Iverson R.M., 1997. The physics of debris flows. Reviews of Geophysics, Vol.35, issue 3, 245-296.
- Johnson, A. M. and McCuen, R. H., 1989. Silt dam design for debris flow mitigation. J. Hydraul. Eng., Vol.115, No.9, 1293-1296.
- Mizuyama T., and Y. Ishikawa., 1988. Technical standard for the measures against debris flow (draft). Technical Memorandum of PWRI, No. 2632.
- Murano Y., 1968. Sabo Engineering. Asakura Shoten (in Japanese).
- Nakagawa, H., Takahashi, T., Satofuka, Y., and Kawaike, K., 1999, 2003. Numerical simulation of sediment disasters caused by heavy rainfall in Camuri Grande basin, Venezuela. Proceedings of the 3rd Conference on Debris-Flow Hazards Mitigation.: Mechanics, Prediction, and Assessment, 671-682.
- Osti, R., and Egashira, S., 2008. Method to improve the mitigative effectiveness of a series of check dams against debris flow. Hydrological processes, Vol.22, 4968-4996.
- Takahashi T., Nakagawa H., Harada, T. and Yamashiki Y., 1992. Routing debris flows with particle segregation, Journal of Hydraulic Engineering. ASCE, Vol. 118, No.11, 1490-1507.
- Takahashi T., 2007. Debris flow: mechanics, prediction and countermeasures. Talyor & fancies/balkema, 1-448.
- 671-682.

(投稿受理：平成 26 年 4 月 18 日)